DOKLADY EARTH SCIENCES, 2025, Vol. 520, No. 1, pp. 29–42

GEOLOGY

FINDING OF NEOARCHEAN (2.71 Ga) CONGLOMERATES IN THE KOSTOMUKSHA IRON ORE PROVINCE: ON THE YOUNGEST ARCHEAN STRATOTECTONIC ASSOCIATION IN THE KARELIAN CRATON

© 2025 A. I. Slabunov[a, *], N. S. Nesterova[a], S. V. Mudruk[a, b], O. A. Maksimov[a], and A. V. Kervinen[a]

Presented by Academician of the RAS Y. A. Kostitsyn July 15, 2024
Received July 15, 2024
Revised September 13, 2024
Accepted September 16, 2024

Abstract. A lens of earlier unknown polymict conglomerates was found in the axis of the Kostomuksha greenstone belt (KGB), Karelian Craton. Their clastic portion consists of poorly graded, largely angular pebbles. They are comparable in composition to rocks from the surrounding greenstone complex, such as: 1) amphibolites similar to KGB's Mesoarchean gabbroic rocks and basalts; 2) magnetite-amphibole quartzites similar to Mesoarchean magnetite-biotite-amphibole quartzites associated with banded iron formation; 3) Neoarchean (2.75 Ga) quartz metagraywacke. The conglomerates are highly deformed ($\gamma > 10$) under conditions of a sinistral shear. The conglomerates were deposited about 2.71 Ga ago, as indicated by analysis of zircons from the matrix. Thus, a new Neoarchean stratotectonic association, the youngest in the greenstone complex, was found in the KGB. It seems to have been formed in a pull-apart basin at the final stage of KGB formation, in which shearing played an important part. Volcanogenic and sedimentary associations of similar age are known in the Khedozero-Bolshozero, Kuhmo and Takanen greenstone belts of the Karelian Craton.

Keywords : *conglomerate, zircons, U-Th-Pb age, Archean, Kostomuksha greenstone belt, Karelian Craton*

DOI: 10.31857/S26867397250104e9

Conglomerates are among the sedimentary rocks that have significant importance for paleotectonic and paleogeographic reconstructions, as they make it possible to judge the composition of rocks in the area of destruction and indicate an active environment in the area of sedimentation. These can be river systems, basins with rapidly eroding shores, including those under the influence of active tectonics. Deformed conglomerates are a classic object for studying the conditions and nature of deformations and their quantitative assessment [1].

Conglomerates are widely developed in the Archean and are known in the sections of many greenstone belts, for example, in the Moodies Group of the classic Barberton belt of the Kaapvaal Craton [2], in the Timiskaming Group of the Abitibi belt in the Superior Province [3], as well as in the greenstone belts of the Karelian Craton of the Fennoscandian Shield [4–7] , including in the Kostomuksha Greenstone Belt (KGB) [8].

The KGB (Fig. 1 a) is located in the central part of the Karelian Craton of the Fennoscandian Shield [9] and hosts the largest iron deposit in NW Russia [10]. The main ore-bearing sequence of the KGB (Gimoly Group) contains at its base the well-known conglomerates of the Sukkozero Formation. However, during the field work of 2022 in this important mining region of the country, previously unknown conglomerates were discovered, to which this article is devoted for their first description.

The stratotectonic section of the KGB includes two stratotectonic associations (STA): Kontokki and Gimoly 10]. The thickness of the greenstone complex section is estimated up to 5.5 km [8]. The Kontokki STA traditionally includes three formations (Fig. 1 a): Niemijarvi (thickness 200–1300 m), composed of metamorphosed tholeiitic

[a] *Karelian Research Centre of the Russian Academy of Sciences, Karelia, Petrozavodsk, Russian Federation*
[b] *Geological Institute of the Kola Science Centre of the Russian Academy of Sciences, Apatity, Russian Federation*
**e-mail: slabunov@krc.karelia.ru*

Table 1. Results of age determination for rocks of the Kostomuksha greenstone belt of the Karelian Craton.

No.	Age, Ma	Interpretation	Rock	Position	Dating method	Reference
Kontokki series						
1	2874±35	magmatic event	komatiites	Ruvinvaara Formation, Kontokki Group	Sm-Nd isochron	Vrevskii, 2022 [11]
2	2843±39	magmatic event	komatiites and basalts	Kontokki Group	Sm-Nd isochron	Puchtel et al., 1998 [11]
3	2813±78	magmatic event	komatiites and basalts	Kontokki Group	Pb-Pb isochron	Puchtel et al., 1998 [11]
4	2808±95	magmatic event	komatiites and basalts	Niemijarvi and Ruvinvaara Formations, Kontokki Group	Sm-Nd isochron	Lobach-Zhuchenko et al., 2000a[11]
5	2795±40	magmatic event	komatiites	Kontokki Group	Re-Os isochron	Puchtel et al., 2001 [11]
6	2837±4.6	detrital magmatic zircon	BIF-1	Ruvinvaara Formation, Kontokki Group	Zr, U-Pb (LA-ICP-MS)	Slabunov et al., 2023[11]
	2748 ±7	metamorphic event				
	1890–1830	metamorphic event				
7	2800±10	magmatic event	rhyolite	Shurlavaara Formation, Kontokki Group	Zr, U-Pb (SHRIMP-II)	[12]
8	2795±10	magmatic event	rhyolite	Shurlavaara Formation, Kontokki Group	Zr, U-Pb (TIMS)	Lobach-Zhuchenko et al., 2000a [11]
9	2792±6	magmatic event	dacitic tuff	Kontokki Group	Zr, U-Pb (SHRIMP-II)	Kozhevnikov et al., 2006[11]
10	2791±23	magmatic event	dacite	Shurlavaara Formation, Kontokki Group	Zr, U-Pb (NORDSIM)	Bibikova et al., 2005a[11]
11	2790 ±21	magmatic event	rhyolitic tuff	Shurlavaara Formation, Kontokki Group	Zr, U-Pb (TIMS)	Bibikova et al., 2005a[11]
12	2757±113	metamorphic event	rhyolite	Shurlavaara Formation, Kontokki Group	Sm-Nd isochron	Puchtel et al., 1998 [11]
13	2810–2790	detrital zircon	BIF-2	Shurlavaara Formation, Kontokki Group	Zr, U-Pb (LA-ICP-MS)	Slabunov et al., 2023[11]
	2725±6	metamorphic event				
	2412±17	metamorphic event				
14	2734 ±3.5	metamorphic event	BIF-2	Shurlavaara Formation, Kontokki Group	Zr, U-Pb (SHRIMP-II)	Slabunov et al. 2023 [11]
15	2729±62	metamorphic event	komatiites and basalts	Kontokki Group	Pb-Pb isochron	Puchtel et al., 1998 [11]
16	2691±5.3	metamorphic event	rhyolite	Shurlavaara Formation, Kontokki Group	Titanite, U-Pb (TIMS)	Bibikova et al., 2001 [11]
17	2688±6.3	metamorphic event	andesite	Kontokki Group	Titanite, U-Pb (TIMS)	Bibikova et al., 2001 [11]

Continuation

No.	Age, Ma	Interpretation	Rock	Position	Dating method	Reference
18	2674±13	metamorphic event	amphibolite	Kontokki Group	Zr, U-Pb (SHRIMP-II)	Levskii et al., 2009 [11]
			Gimoly Group			
19	2759±8.9	magmatic event	rhyolite	Kostomuksha Formation, Gimoly Group	Zr, U-Pb (SHRIMP-II)	[13]
20	3146–2770	detrital zircon	graywacke	Kostomuksha Formation, Gimoly Group	Zr, U-Pb (SHRIMP-II)	[13]
	2753±15	detrital zircon	graywacke	Kostomuksha Formation, Gimoly Group	Zr, U-Pb (SHRIMP-II)	[13]
21	2743 ±15	magmatic event	rhyolite	Kostomuksha Formation, Gimoly Group	Zr, U-Pb (SHRIMP-II)	[13]
22	2910±12	detrital zircon	BIF-3	Kostomuksha Formation, Gimoly Group	Zr, U-Pb (LA-ICP-MS)	[11]
	2753±4	detrital zircon				
	2720±2.9	metamorphic event				
	2652±5	metamorphic event				
	2560	metamorphic event				
	2452±12	metamorphic event				
23	2978±24	detrital zircon	BIF-3	Kostomuksha Formation, Gimoly Group	Zr, U-Pb (SHRIMP-II)	Slabunov et al., 2023 [11]
	2914±7	detrital zircon				
	2786±55	detrital zircon				
	2732±5	metamorphic event				
	2639±7	metamorphic event				
	1855±8	metamorphic event				
			Neoarchean conglomerates			
24	**2749±3**	detrital zircon	clast in conglomerate		Zr, Pb-Pb (LA-ICP-MS)	present study
25	**2716±15**	detrital zircon (MDA)	Conglomerate matrix		Zr, U-Pb (LA-ICP-MS)	present study
	2668±21	metamorphic event				
			Intrusions			
26	2797±5	magmatic event	TTG	intrusion	Zr, U-Pb (NORDSIM)	Bibikova et al., 2005a [11]

Ending

No.	Age, Ma	Interpretation	Rock	Position	Dating method	Reference
27	2788±13	magmatic event	TTG	intrusion	Zr, U-Pb (NORDSIM)	Bibikova et al., 2005a[11]
28	2782±5	magmatic event	TTG	intrusion	Zr, U-Pb	Samsonov, 2004[11]
29	2747±17	magmatic event	TTG	intrusion	Zr, U-Pb (TIMS)	Bibikova et al., 2005a [11]
30	2719±6	magmatic event	granodiorite	sanukitoid intrusion	Zr, U-Pb (NORDSIM)	Bibikova et al. 2005b [11]
31	2712 ± 9	magmatic event	granodiorite	sanukitoid intrusion	Zr, U-Pb (NORDSIM)	Bibikova et al., 2005b [11]
32	2707 ± 9	magmatic event	diorite	sanukitoid intrusion	Zr, U-Pb (NORDSIM)	Bibikova et al., 2005b [11]
33	2707 ± 31	magmatic event	granite-porphyry	intrusion	Zr, U-Pb (TIMS)	Lobach-Zhuchenko et al., 2000a [11]
34	2679±8	magmatic event	microcline granite	intrusion	Zr, U-Pb (TIMS)	Lobach-Zhuchenko et al., 2000a [11]
35	2635±11	metamorphic event	granite-porphyry	intrusion	Titanite, U-Pb (TIMS)	Nesterova et al., 2011 [11]
36	2404±5	magmatic event	dolerite	dyke	baddeleyite, U-Pb (TIMS)	Stepanova et al., 2017 [11]
37	2132±33	magmatic event	dolerite	dyke	Sm-Nd isochron	Stepanova et al., 2014 [11]
38	1200	magmatic event	kimberlites and lamprophyres	dyke	Rb-Sr isochron	Nikitina et al., 1999 [11]

basalts with rare interlayers of komatiites and magnetite quartzites; Shurlovaara (thickness up to 600 m), represented by felsic volcanics with interlayers of banded iron formations (banded iron formation – BIF); Ruvinvaara (thickness up to 1300 m), composed of metabasalts and komatiites with felsic differentiates, as well as with interlayers of schists and BIF. The age of the (rhyolite)-basalt-komatiite sequence of the Kontokki STA is estimated at 2.87–2.84 Ga, while the age of felsic volcanics with interlayers of BIF (Shurlovaara Formation) is 2.81–2.78 Ga (Table 1).

The Gimoly STA, with widely varying thickness (180-2300 m), is composed of metasediments and volcanics. At its base, conglomerates (Sukkozersk Formation) up to several meters thick are identified. The clastic portion of these conglomerates consists of granitoids, and also contains felsic volcanics comparable in composition to the rocks of the Shurlavaara Formation. Metasediments of this sequence are represented by flyschoid-type graywackes [14] with thick interlayers of BIF-3, whose proportion decreases eastward. An integral part of the section includes Neoarchean (2.76–2.74 Ga) felsic volcanics – helleflintas (Table 1), analogues of which are the main source material for graywackes ([13] and references therein). The close relationship between felsic volcanics and metagraywackes has been established based on rock geochemistry studies [14], but is also emphasized by zircon data. Zircons from graywacke predominantly (70% of the sample) consist of crystals whose morphology, structure, geochemistry, and age are analogous to those from helleflinta [13].

The greenstone belt is surrounded by Neoarchean (2.78–2.75 Ga) granitoids of the tonalite-trondhjemite-granodiorite (TTG) association (Fig. 1a), and it is also intersected by several generations of Neoarchean granites and granodiorites (sanukitoids), Paleoproterozoic gabbroid dykes and Mesoproterozoic bodies of lamproites and kimberlites (Table 1).

The evolution of the KGB structure [16] suggests that the greenstone complex underwent multiple

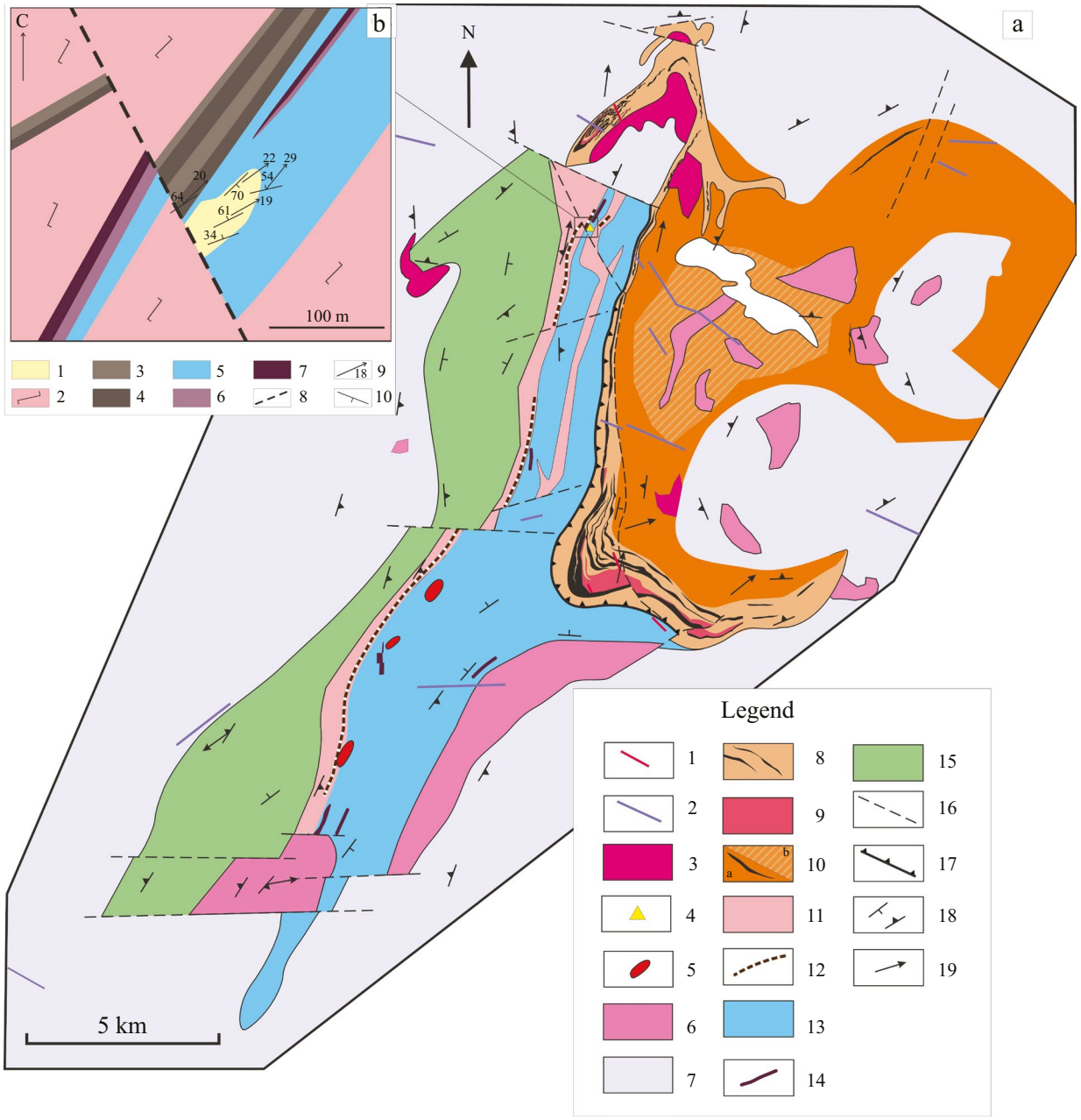

Fig. 1. Geological structure scheme (a) of the Kostomuksha greenstone belt ([11, 15], with the authors' additions) and (b) detailed area with a lens of Neoarchean (2.71 Ga) conglomerates. (a): *1* – Neoproterozoic (1.2 Ga) lamproites and kimberlites (Table 1), *2* – Paleoproterozoic (2.40 and 2.14 Ga) dolerites (Table 1); *3–9* Neoarchean (Table 1): *3* – 2.68 Ga granites; *4* – 2.71 Ga polymictic conglomerates; 5 – 2.71 Ga sanukitoids; 6 – 2.72 Ga granites; *7* – 2.78 Ga granitoids of TTG association; *8–10* – rocks of the Gimoly STA (Table 1): *8* – 2.76-2.74 Ga metagreywackes with BIF-3 interlayers; *9* – 2.76–2.74 Ga sills and dykes of metarhyolites (helleflintas); *10* – metasediments of the Surlampi Formation with BIF interlayers: a – weakly and b – strongly migmatized; *11–14* – Mesoarchean (2.87-2.78 Ga) (Table 1): *11* – tuffs, rhyolite tuffites (Shurlovaara Formation); *12* – BIF-2 interlayers; *13* – komatiite-basalt complex with dacites (Ruvinvaara Formation); *14* – BIF-1 interlayers; *15* – basalts and komatiites (Niemijarvi Formation); *16* – faults; *17* – thrust; *18* – *19* – bedding elements: *18* – banding and gneissosity, *19* – mineral lineation. (b): *1* – 2.71 Ga polymictic conglomerates; *2–4* – Mesoarchean (2.80–2.78 Ga) rocks of Shurlovaara Formation: *2* – felsic volcanics, *3* – BIF-2 interlayers; *4* – schist interlayers; *5–7* – Mesoarchean (2.87–2.81 Ga): *5* – komatiite-basalt complex with dacites (Ruvinvaara Formation), *6* – BIF-1 interlayers, *7* – interlayers of barren quartzites and schists; *8* – faults; *9–10* – bedding elements: *9* – mineral lineation, *10* – banding and gneissosity.

deformation events (D1-5): the early stage (D1) was accompanied by the formation of isoclinal folds with horizontal hinges and lineation; the second stage (D2) involved multi-phase NE-trending folding, associated with sinistral shear, while D2 stage folds are characterized by schistosity and mineral lineation parallel to their axial surfaces and hinges respectively; later stages D3-5 manifested as faults: D3 – in the northern part of the belt as NW-trending faults and dextral shears, D4 – meridional faults and tectonic breccia zones, D5 – system of sublatitudinal faults with a strike–slip component.

The greenstone complex KGB underwent metamorphic transformations under epidote-amphibolite to amphibolite facies conditions [8] at 2.72, 2.69 Ga (Table 1) (the latter being most significant), as well as in certain zones under lower parameters at 2.42 and 1.89 Ga (Table 1) ([10, 11] and references therein). The early deformation stage D1 corresponded to amphibolite facies conditions, D2 – to epidote-amphibolite to amphibolite facies conditions, while albite-chlorite metasomatites formed during the later stages [16].

A previously unknown conglomerate body (Fig. 1b) was discovered among basalts with BIF lenses of the Kontokki STA (Ruvinvaara Formation), with felsic volcanics containing BIF interlayers of the Shurlovaara Formation located in their immediate vicinity. The conglomerate body can be traced along strike for approximately 80 m, with a width of about 50 m (Fig. 1b). The direct contact between conglomerates and underlying metabasalts is exposed in a very small area, which prevents detailed study, however, the relationship between banding orientations in conglomerates and schistosity in surrounding rocks indicates that this contact is tectonized. Squeezing and significant stretching of pebbles parallel to fold hinges and lineation, as will be discussed below, support this conclusion.

Structural features of conglomerates. The studied conglomerates display layering (Fig. 2a), expressed in alternating layers with cement of different colors, as well as variations in pebble composition and orientation. Bedding is deformed into compressed with mean orientation of hinge line is NE (55°/19°) [17].

The wings of the fold are complicated by additional minor folds, whose average hinge orientation is also close to the orientation of the main fold hinge. Mineral lineation along amphibole is parallel to the hinges of both large and small folds.

The size of the clastic component of conglomerates varies from 1–2 cm to 40 cm, i.e., from pebbles to boulders (Fig. 2a–d), with all fragments significantly elongated parallel to lineation (Fig. 2a, d). In the plane perpendicular to lineation, it is clearly visible that fragments of mafic composition typically have an elliptical shape with smoothed contours, while quartzite fragments are often angular (Fig. 2 c, d). These observations indicate that elongated pebbles form classical stretching lineation. Analysis of pebble morphology suggests significant planar deformation ($K \approx 1$; $\gamma > 10$) under simple shear conditions with sinistral movement along the trajectory NE 55°/23° along steep NE-trending shear planes [17].

The orientation of folds and sinistral simple shear deformation of conglomerates correspond to NE-trending folds and sinistral shear zones of stage D2 of the structural-age scale constructed by V.N. Kozhevnikov for the KGB [16].

Petrographic features of conglomerates. The studied conglomerates belong to the polymictic type: their fragments consist of amphibolites (metagabbroids and metabasites) with various structures and textures and a wide range of quartzites (Fig. 2b).

Amphibolites from conglomerate fragments vary from leucocratic to melanocratic, characterized by spotted texture, porphyroblastic and granonematoblastic structure. Porphyroblasts are represented by amphibole. The groundmass consists of plagioclase and amphibole. Mineral composition of the rock: plagioclase (10–55%), amphibole (30–90%), epidote (up to 6%), titanite (up to 4%), magnetite (up to 1%), quartz (less than 1%). *Plagioclase* is represented by hypidiomorphic grains with concentric zoning, less commonly by unzoned grains with polysynthetic twins. Compositionally, plagioclase corresponds to andesine. In zoned grains, the anorthite component content changes from 45 to 30% from core to rim. Among plagioclase grains, probably relicts of magmatic origin have been preserved. Its metamorphic transformation is manifested in epidote replacement and desilication (to oligoclase). *Amphibole* occurs both as large porphyritic segregations (up to 2mm) and as small individual grains (up to 0.3 mm) or their aggregates in the rock matrix. Large porphyroblasts contain titanite inclusions. All studied amphiboles compositionally correspond to magnesian hornblende. *Epidote* develops after primary plagioclase. Individual xenomorphic grains or intergrowths of several grains are observed, which often contain quartz inclusions. Grain boundaries are often rimmed by amphibole. *Titanite* forms lenticular intergrowths of several grains or can form

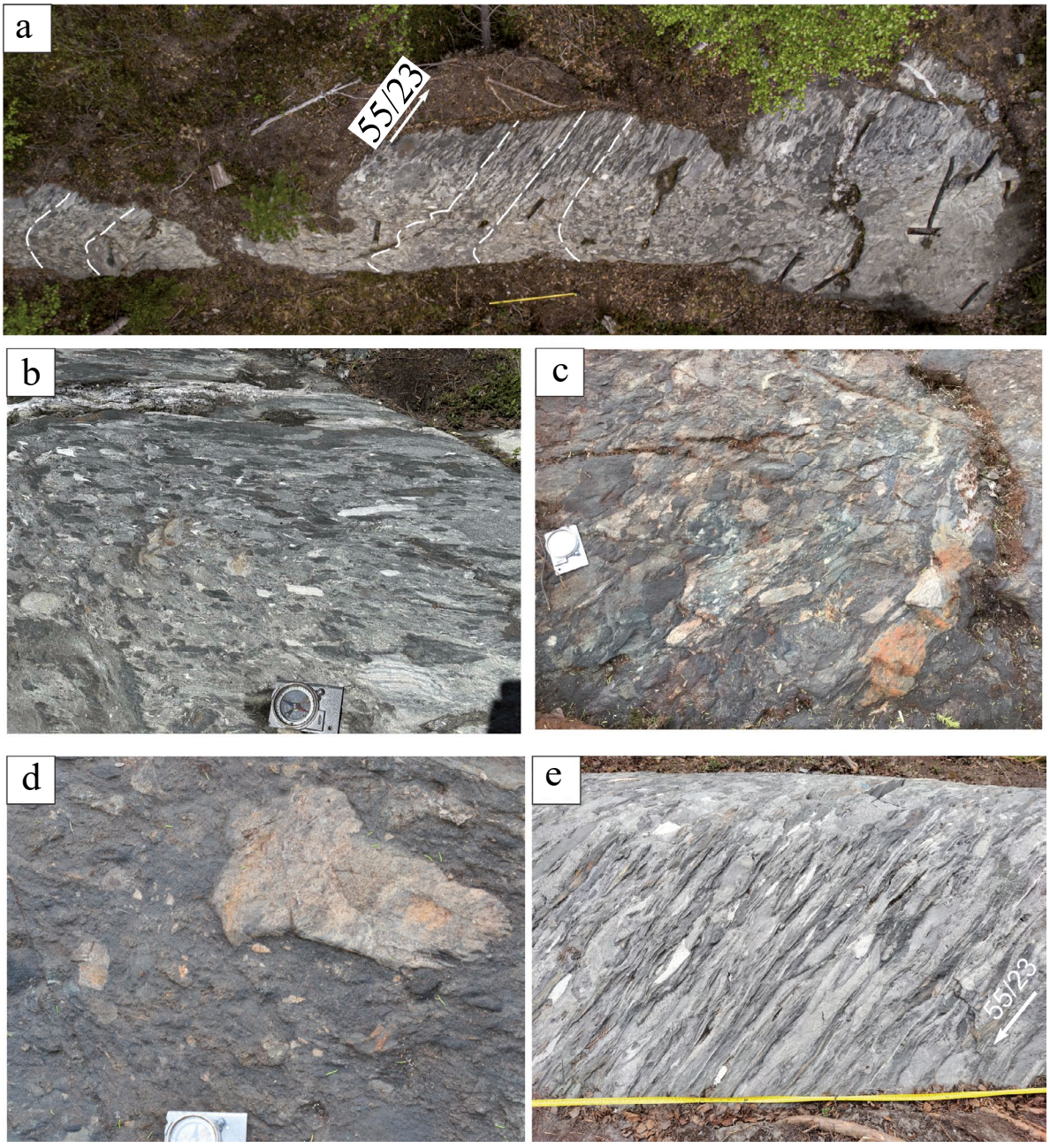

Fig. 2. Neoarchean (2.71 Ga) conglomerates of the Kostomuksha greenstone belt in outcrop: (a) general view of the outcrop (scale – yellow measuring tape 1 m), dotted line – structural lines, arrow – average orientation of lineation plunge (NE 55° at angle 23°); (b) conglomerates with ellipsoidal fragments of metabasites, banded quartzites – quartz graywacke, banding is visible in the rocks, photo plane is suborthogonal to the schistosity surface (scale – compass 10 cm); (c) conglomerates with angular and ellipsoidal fragments of amphibolites (metabasalts), metabasalts with plagioclase porphyries, quartz metagraywacke (scale – compass 10 cm); (d) large fragment of deformed quartz metagraywacke (scale – compass 10 cm); (e) conglomerates in a plane orthogonal to the schistosity surface and parallel to lineation, arrow – orientation of lineation plunge (NE 55° at angle 23°).

thin layers in the rock matrix. Titanite overgrowth around magnetite is observed.

Light-colored conglomerate fragments are represented by various quartzites and quartz metagreywackes. A typical rock of such fragments is a banded magnetite-amphibole quartzite with grano-nematoblastic texture. The rock consists of closely adjacent isometric quartz grains, among which amphibole and magnetite grains are evenly distributed. Additionally, thin (about 1 mm) magnetite-amphibole layers are observed in the rock.

Quartz makes up the bulk of the rock (up to 75–80%). In leucocratic layers, quartz is distinguished by larger grain size up to 1 mm. In amphibole-magnetite bands, grain size does not exceed 0.3 mm. *Amphibole* (comprises about 15% of the rock) is represented by elongated prismatic grains with pleochroism from light green to dark green. Together with magnetite, it forms darker layers in quartzites, where amphibole overgrowth around magnetite can be traced. *Magnetite* comprises about 10% of the rock volume, forms rounded grains 0.1-0.2 mm in size and is evenly distributed in the rock.

Among the fragments of quartzites in conglomerates, varieties are also noted where plagioclase plays a significant role, and they can be classified as quartz greywackes. The mineral composition of such rocks (for example, sample E-KS22-34-5a): quartz – 62%, amphibole – 25%, plagioclase – 8%, magnetite – 4%, pyrite – 1%. *Plagioclase* is observed as small xenomorphic grains of andesine-oligoclase composition. They are not zonal and do not have polysynthetic twins.

In terms of petrographic characteristics, these rocks are similar to low-ore quartzites associated with Mesoarchean BIF [15].

The cement of conglomerates constitutes 30–40% of the rock volume and is represented by gray and light-gray fine-grained rock with schistose texture and grano-nematoblastic structure. These schists show wide variations in dark-colored minerals content. In melanocratic varieties, amphibole content reaches 50%, quartz – 20%, plagioclase – 20%, chlorite – 5%, biotite – 5%. *Amphibole* is represented by elongated grains of magnesian and ferrous hornblende. Large grains contain inclusions of carbonate and quartz. *Chlorite and biotite* often occur in intergrowths with amphibole.

In more leucocratic variety of cement, plagioclase predominates – 33% and quartz – 40%, dark-colored minerals are mainly represented by hornblende – 17%, chlorite – 6%, and biotite – 4%. Accessory minerals include grains of zircon, titanite, calcite, and ore mineral.

Petrogeochemical characteristics of conglomerate clasts. By chemical composition (Table 2), basic rock clasts from conglomerates correlate well with basalts of the Kontokki STA (Fig. 3a), which is particularly evident in spider diagrams of normalized REE content (Fig. 3b). A slight enrichment of amphibolite fragments relative to the basic rocks sample of the Kontokki STA in light REEs and wider variations in the composition of petrogenic oxides may be associated with both the predominance of basalts in the control sample and more differentiated gabbroids in the fragments, as well as with the influence of superimposed processes. Fragments of quartzites and quartz graywackes are distinguished by high silica content and low – K_2O+Na_2O, which distinguishes them from felsic volcanics of KGB but relates them to quartzites associated with BIF. Geochemical characteristics of quartzites from conglomerate fragments (Fig. 3c, d) make it possible to more confidently correlate this group with the latter [15]. Among them, two subgroups are distinguished by the degree of REE differentiation (Fig. 3d): the first is differentiated ($La_N/Yb_N = 9 - 19$), the second is weakly differentiated ($La_N/Yb_N = 1 - 2$). The rocks of the first subgroup correlate well with Mesoarchean low-ore quartzites [15], while compositions with such weakly differentiated REEs are noted among metagraywackes of the Gimoly STA.

Based on the presented geological data, the studied conglomerates formed later than the Mesoarchean (2.87–2.84 Ga) basic rocks and possibly the Neoarchean (2.75–2.74 Ga) rocks of the Gimoly STA, since rocks similar in composition to the latter were found in fragments, but preceded intense deformations that were probably associated with accretionary processes dated at 2.72 and 2.69 Ga [11].

U – Th – Pb geochronology of zircons from conglomerates. For a more reliable age assessment of the discovered conglomerates, zircons extracted from the cement and from one of the fragments were studied. U – Th – Pb dating of zircon from the cement (120 analytical points) and from the fragment (60 points) was performed by LA-ICP-MS at the Laboratory of Chemical-Analytical Research of the the Geological Institute, Russian Academy of Sciences (GIN RAS, Moscow, Russia), using the approved methodology ([11] and references therein). For quality control of the analyses, zircon standards 91500 and Plesovice with standardized ages of 1062.4±0.4 and 337.1±0.4 Ma, respectively, were used. During the study of samples E-K22-34-2 and E-KS22-34-5a, the weighted mean $^{206}Pb/^{238}U$ age estimates (±2σ) obtained for the control standards were 1067±14.8 (n =12) and 1069±7.4 (n =6) Ma and 335.2±5.8 (n =12) and 337.7±5.8 (n =12) Ma, respectively, which agrees well with the reference values. The Isoplot 4.15 program [18] was used for graphical illustration of the obtained results.

From sample E-K22-34-2 (conglomerate cement), collected at point 64°46'10'' N, 30°40'09'' E, weighing about 700 g, more than

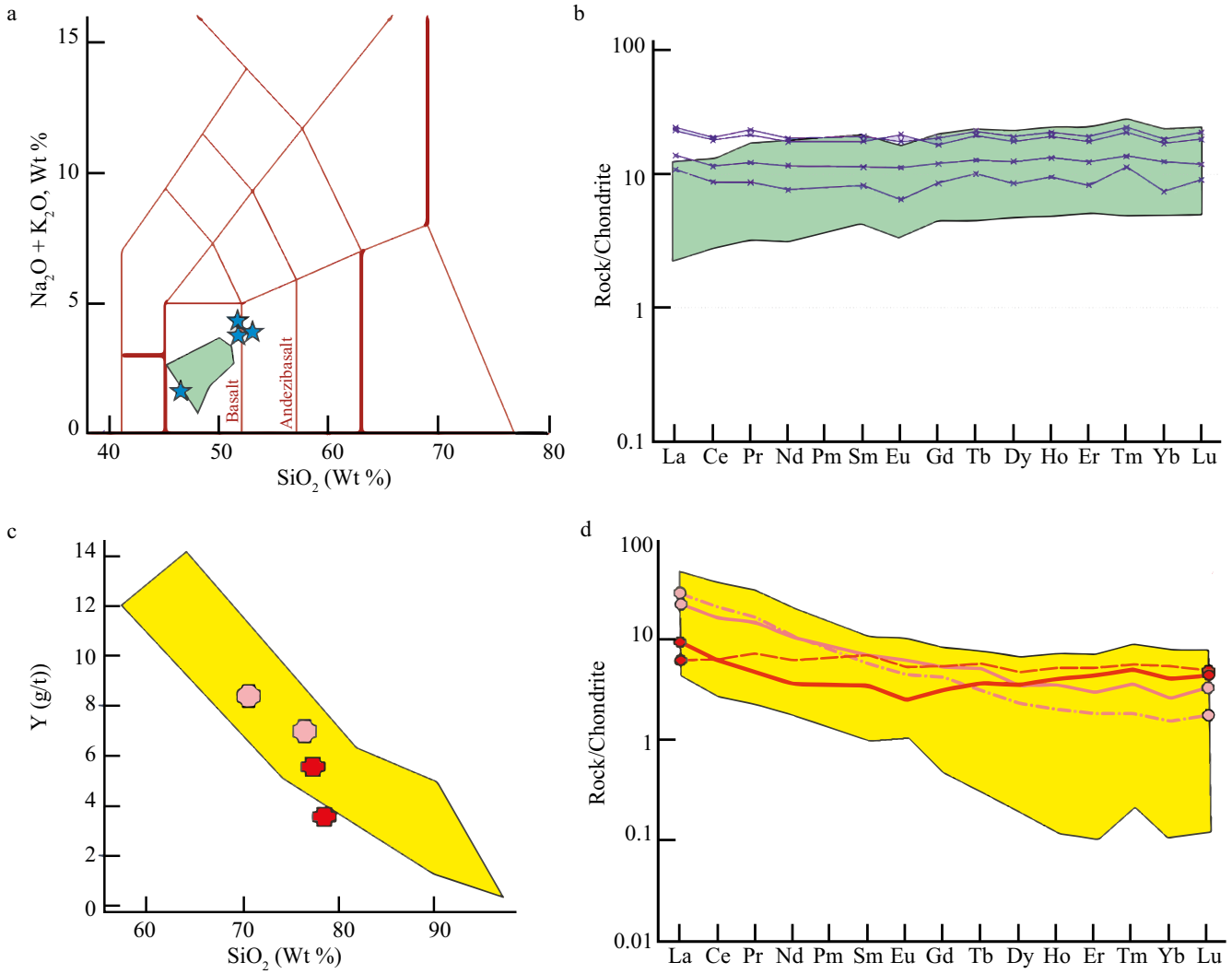

Fig. 3. Figurative points of amphibolite compositions (blue asterisks) (a, b), quartzites (pink symbols) – quartz graywacke (red symbols) (c, d) from conglomerate clasts on diagrams SiO_2-Na_2 +K_2O (a), SiO_2-Y (c) and chondrite-normalized REE patterns (b, d), green fields – composition of Mesoarchean basalts of KGB, yellow fields – compositions of Mesoarchean quartzites associated with BIF [15].

Table 2. Chemical composition (oxides in wt.%, elements in ppm) of fragments in Neoarchean (2.71 Ga) conglomerates of the Kostomuksha greenstone belt

	1	2	3	4	5	6
SiO_2	70.52	78.69	76.36	52.22	50.72	45.08
TiO_2	0.28	0.19	0.14	1.15	1.35	0.72
Al_2O_3	7.8	9.98	2.79	16.8	17.19	11.59
Fe_2O_3	1.21	0.47	3.16	1.05	1.02	1.9
FeO	7.39	2.15	6.75	8.48	7.39	13.06
MnO	0.164	0.076	0.125	0.223	0.187	0.436

Ending

	1	2	3	4	5	6
MgO	4.34	0.37	2.42	4.85	5.23	11.23
CaO	5.36	4.32	2.74	9.82	11.1	12.04
Na_2O	1.09	2.35	0.22	3.56	4.03	1.02
K_2O	0.16	0.11	0.11	0.28	0.21	0.46
P_2O_5	0.015	0.02	0.02	0.07	0.1	0.05
H_2O	0.26	0.04	0.72	0.11	0.05	0.13
LOI	0.96	0.98	4.25	1.26	1.31	2.06
Li	5.89	2.83	5.79	9.40	7.10	18.55
Sc	9.34	3.52	3.66	58.89	46.62	37.49
V	80.52	34.12	34.88	395.74	375.63	266.60
Cr	223.26	79.48	146.84	144.61	331.51	1513.63
Co	54.42	4.81	37.10	47.27	36.79	75.21
Ni	66.50	12.70	42.83	100.28	96.88	533.36
Cu	802.37	21.61	1281.09	13.22	22.41	22.57
Zn	59.92	36.45	40.24	100.68	75.94	160.12
Rb	1.67	3.48	2.76	3.50	5.89	4.78
Sr	50.64	117.23	5.92	211.93	246.74	18.17
Y	8.36	3.57	6.90	19.33	27.80	13.82
Zr	50.60	93.03	21.95	55.10	81.76	34.59
Nb	1.97	2.58	1.03	2.96	4.44	1.72
Ba	55.19	205.06	19.57	191.36	216.56	78.99
La	1.99	9.31	3.04	4.56	7.03	3.57
Ce	5.31	17.78	5.27	9.93	15.54	7.56
Pr	0.79	1.83	0.52	1.37	2.21	0.97
Nd	3.81	6.67	2.23	7.30	11.03	4.80
Sm	1.39	1.14	0.69	2.30	3.59	1.67
Eu	0.40	0.34	0.19	0.86	1.53	0.50
Gd	1.47	1.13	0.84	3.32	4.57	2.37
Tb	0.26	0.14	0.17	0.60	0.92	0.47
Dy	1.60	0.77	1.20	4.27	6.05	2.92
Ho	0.35	0.14	0.28	0.93	1.34	0.67
Er	1.15	0.40	0.96	2.78	3.95	1.87
Tm	0.17	0.05	0.15	0.41	0.62	0.34
Yb	1.17	0.33	0.87	2.73	3.74	1.63
Lu	0.16	0.06	0.15	0.40	0.62	0.31
Hf	1.46	2.24	0.75	2.20	3.00	1.39
Ta	0.17	0.22	0.24	0.33	0.39	0.17
Pb	1.91	3.29	1.09	6.18	8.20	1.86
Th	1.99	2.51	1.40	0.40	0.71	0.45
U	0.40	0.46	0.22	0.12	0.22	0.21

Note. 1 – E-K22-34/5a, plagioclase-magnetite-amphibole quartz graywacke (with predominant zircons aged 2749 Ma); 2 – E-K22-34/4, amphibole-biotite quartzite; 3 – E-K22-34/1, quartzite with sulfides; 4 – E-K22-34/3B, amphibolite (metagabbro); 5 – E-K22-34/6A, amphibolite (metagabbro); 6 – E-K22-34/8B, amphibolite. Major elements were determined by classical chemical silicate analysis method, and trace elements – by ICP MS method (X Series II, ThermoScientific) with dissolution in autoclaves at the Analytical Laboratory of the Institute of Geology, resource sharing center, Karelian Research Center RAS (Petrozavodsk).

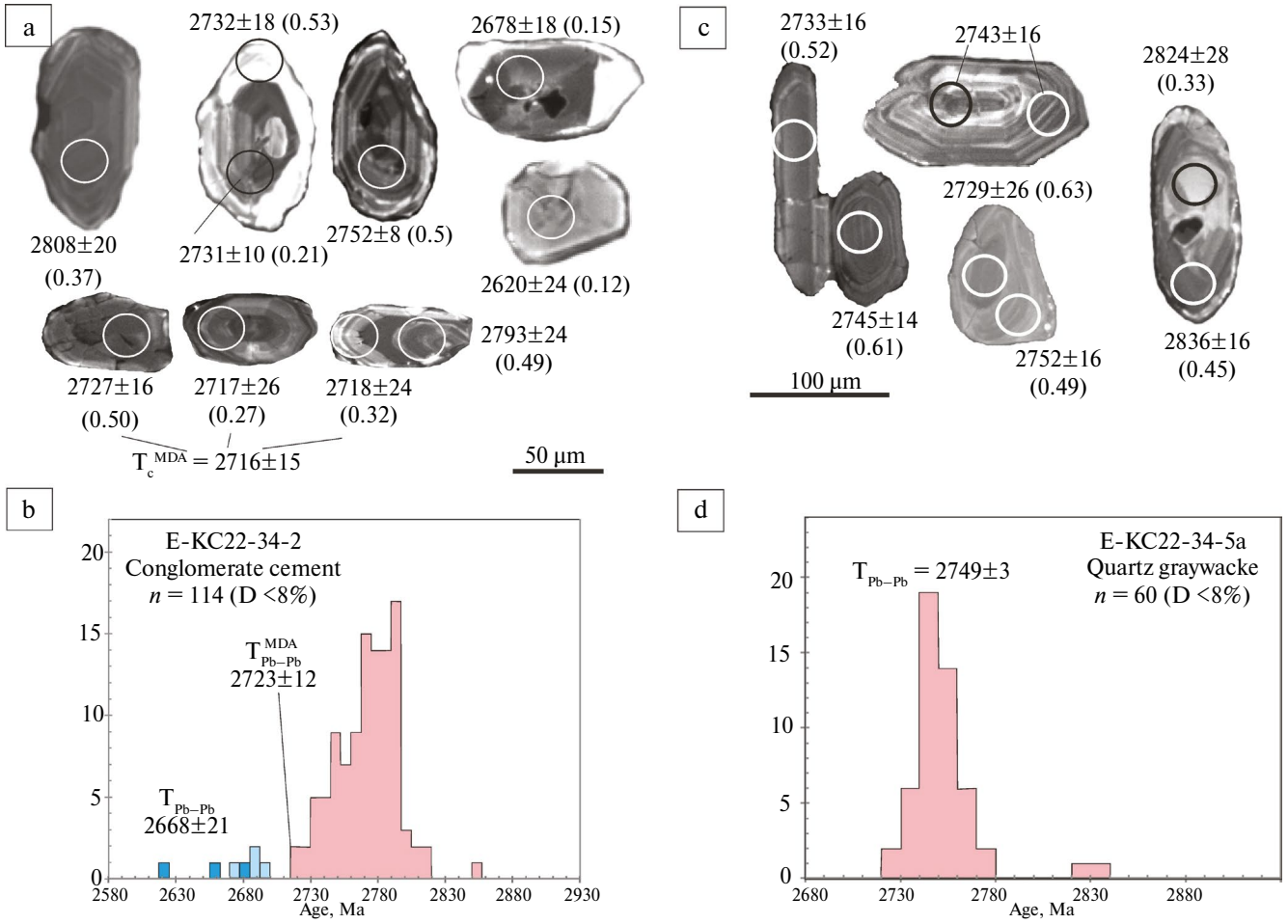

Fig. 4. Grain structure (a, c) and isotopic age (determined by LA-ICP-MS, *n* – number of analytical points, D* – discordance in %) of zircon from conglomerate cement (b) and quartz greywacke fragment (d) : (a, c) cathodoluminescent image of zircons from cement (a) and fragment (c) of conglomerate, circles – location of analytical dating points and their values $T_{Pb\text{-}Pb}$ in Ma (1σ), in brackets – Th/U ratio; (b, d) histograms of ^{207}Pb – ^{206}Pb ages ($T_{Pb\text{-}Pb}$) of zircon from cement, $T^{MDA}_{Pb\text{-}Pb}$ – ^{207}Pb – ^{206}Pb age of three youngest grains (MDA – maximum depositional age). * D=100×(T (^{206}Pb/ ^{238}U)/ T (^{207}Pb/ ^{206}Pb)-1)

300 zircon grains were extracted. They are represented by yellowish-brown colored crystals of prismatic habit: from short- to long-prismatic with Ke – 1:2, 1:3, ranging in size from 40 to 150 μm (Fig. 4a). Based on internal structure, two morphological types can be distinguished among zircons in this sample. Grains of the first type, which strongly predominate, are characterized by distinct fine oscillatory zoning and Th/U ratio significantly greater than 0.2 (Fig. 4a), which is characteristic of magmatic zircon. Grains of the second type show signs of patchy zoning (Fig. 4a) and Th/U ratios for most of them are less than 0.2, which is typical for metamorphogenic zircon. Moreover, in zircons of both morphotypes, there are grains with light rims (Fig. 4a), which may indicate the presence of late metamorphogenic processes that cannot be dated in this sample.

^{207}Pb – ^{206}Pb age ($T_{Pb\text{-}Pb}$) of zircons of the first morphological type varies from 2.86 to 2.717 Ga with a complex polymodal distribution of values (Fig. 4 c). $T_{Pb/Pb}$ of the three youngest zircon grains from this sample (2717±26 (discordance in % (D) = 0.01); 2718±24 (D = –0.01); 2727±16 (D = –2.5), Fig. 4a bottom row) is estimated at 2723±12 Ma (Fig. 4b). Similar estimates are obtained when calculating U – Pb concordant age (T_c) from these three points – 2716±15 (MSWD = 1.9) Ma. This figure is most accurate for estimating the maximum age of conglomerate sedimentation. $T_{Pb\text{-}Pb}$ of metamorphogenic zircons of the second morphological type, with discordance less than 5%, falls within the interval of 2.62–2.70 Ga and

is estimated at 2668±21 Ma based on 7 points. Meanwhile, T_c for the 5 most concordant points from this sample is 2672±12 (MSWD = 0.023) Ma.

Thus, the age of conglomerate sedimentation falls within the interval of 2716±15 – 2672±12 Ma. Its most probable estimate corresponds to the area of minimum density of analytical points between the two main peaks on the age distribution histogram (Fig. 4b) and is estimated at approximately 2.71 Ga.

The second sample for geochronological studies of conglomerates was taken from a quartz metagreywacke fragment (sample E-KS22-34-5a). From this 800 g sample, 250 zircon grains were separated. Their study showed that they are represented by transparent brown-colored idiomorphic crystals of elongated prismatic habit with elongation coefficient 1:2, 1:3, rarely 1:4 (Fig. 4c). These crystals are characterized by relatively high idiomorphism and diversity of morphological forms. Among them are prismatic, short-prismatic and isometric crystals of relatively large size (70–180 μm). The internal structure of all studied zircons is very similar and characterized by fine oscillatory zoning (Fig. 4c), their Th/U ratio varies from 0.2–1.1 (average 0.7), suggesting their original magmatic nature.

The distribution pattern of $T_{Pb\text{-}Pb}$ zircon in the histogram (it falls within a narrow range of 2.73–2.77 Ga) (Fig. 4 d), as well as the uniformity of its structural features, indicates the homogeneity of the sample. $T_{Pb\text{-}Pb}$ zircon population, comprising 97% of the total sample, is estimated at 2749±3 Ma (Fig. 4d), which within error margins coincides with its U – Pb-age at the upper intersection of discordia with concordia – 2748±3.5 (MSWD = 0.62) Ma. Additionally, among the studied zircons, a grain was identified with $T_{Pb/Pb}$ values of 2836±16 and 2824±28 Ma (D = –0.11 and –0.35) in two analytical points, respectively (Fig. 4b). Thus, the main source of material detritus (including zircon) during the formation of quartz metagreywacke from the conglomerate fragment is felsic igneous rocks aged 2749±3 Ma. Comparable age (2759 – 2743 Ma, [13]) is characteristic of rhyolites from the Gimoly STA (Table 1), which probably constitute the main source of detritus for sediments of this sequence. Additionally, Mesoarchean felsic igneous rocks contributed a small portion to the quartz metagreywacke composition. Thus, the quartz metagreywacke fragment shows similarities with greywackes of the Gimoly STA in terms of morphology and detrital zircon age, which formed nearly synchronously with Neoarchean (2.75– 2.74 Ga) dacites and BIF of this STA (Table 1) [11, 13].

FORMATION CONDITIONS

Thus, the Neoarchean (2.71 Ga) polymictic conglomerates found in the KGB consist of fragments of surrounding metabasalts, Kontokki STA quartzites, and Gimoly STA quartz greywacke. Importantly, no zircons older than 2.85 Ga (with discordance less than 10%) were found in the cement. The fragments are poorly sorted, and angular fragments are common alongside rounded ones (Fig. 2). All these facts indicate that the conglomerate sequence formed in a basin that received local poorly sorted detrital material. The morphology of the fragments indicates that they were deformed under sinistral simple shear conditions. Considering the composition characteristics, structure, and subsequent deformation conditions, it can be suggested that the conglomerates mark a pull-apart type basin.

MAIN CONCLUSIONS

1. In the axial part of the KGB among metabasalts of the Kontokki STA, a lens of previously unknown polymictic conglomerates was identified, whose clastic component consists of 1) metamorphosed basic rocks comparable in composition to Mesoarchean gabbroids and basalts of the KGB; 2) magnetite-amphibole quartzites comparable to Mesoarchean quartzites associated with BIF; 3) quartz metagreywacke comparable in composition and zirconology to sediments of the Neoarchean Gimoly STA.

2. The age of sedimentation of the discovered conglomerates based on the study of zircon from the cement is definitely younger than 2716±15 Ma and older than 2672±12 Ma, estimated at approximately 2.71 Ga. These data show that a new youngest among Archean STA has been established in the KGB. It is comparable in age to volcanics (2712–2703 Ma) of Khedozero-Bolshezero [12], Takanen (2706 Ma) [19] and sediments (<2.70 – 2.73 Ga) of Kuhmo [20] greenstone belts of the Karelian craton.

3. The studied conglomerates are intensely deformed under conditions of sinistral simple shear along the steep NE-trending planes.

4. The formation of late Neoarchean conglomerates of the KGB probably occurred in a pull-apart basin at the final stage of belt formation under shear deformation conditions. Under such

conditions, the well-known Timiskaming-type conglomerates of the Abitibi greenstone belt of the Superior Province were formed, which are associated with large gold deposits [3] .

ACKNOWLEDGEMENTS

The authors express their gratitude to GIN RAS (Moscow) staff K.G. Erofeeva and A.S. Dubensky for conducting zircon dating work and consultations on using the results. The authors are grateful to Academician N.S. Bortnikov and the second reviewer of the manuscript for valuable comments and remarks that helped improve the article.

FUNDING

This work was financially supported by the RSF (grant No. 22-17-00026)

REFERENCES

1. *Ramsay J.G.* Folding and fracturing of rocks. McGraw-Hill, New York. 1967. 580 p.
2. *Brandl G., Cloete M., Anhaeusser C.R.* Archaean Greenstone Belt. In: The Geology of South Africa. Johnson M.R, Anhaeusser C.R., Thomas R.J. (Eds). The Geologly of South Africa. Geologica Sociely of South Africa, Johannesburg/Council for Geoscience, Pretoria. 2006. Pp. 9–56.
3. *Jackson S.L., Fyon J.A.* The Western Abitibi Subprovince in Ontarion. In: Geology of Ontario. Thurston P.C., Williams H.S., Sutcliffe R.H., Stott G.M. (Eds). Special Vol. 4, Part 1. Ontario Ministry of Northern Development and Mines, 1991. Pp. 405–484.
4. *Chernov V.M* . Stratigraphy and Sedimentation Conditions of Volcanogenic (Leptitic) Iron-Siliceous Formations of Karelia. Moscow-Leningrad: Nauka. 1964. 104 p.
5. *Svetov S.A., Svetova A.I. et al.* Neoarchean Pull-Apart Basins of the Central Karelian Terrane: Rock Sequences and Lithogeochemical Characteristics // Geology and Mineral Resources of Karelia. Issue 8. Petrozavodsk: KarRC RAS. 2005. Pp. 5–17.
6. *Piirainen T* . The geology of the Archaean greenstone-granitoid terrain in Kuhmo, eastern Finland // Archaean geology of the Fennoscandian Shield. Geol. Surv. Finland Spec. Pap.1988. No. 4. Pp. 39–51.
7. *Sorjonen Ward P.* An overview of structural evolution and lithic units within and intruding the late Archean Hattu schist belt, Ilomantsi, eastern Finland. In: Nurmi, P. A. & Sorjonen-Ward, P. (eds.) / Geological development, gold mineralization and exploration methods in the late Archean Hattu schist Belt, Ilomantsi, Eastern Finland. Geol. Surv. of Finland. Spec. Paper. 17. 1993. Pp. 9–102.
8. *Gorkovets V.Ya., Raevskaya M.B., Volodichev O.I. et al.* Geology and Metamorphism of Iron-Siliceous Formations in Karelia. Leningrad: Nauka; 1991. 176 p.
9. *Kulikov V.S., Svetov S.A., Slabunov A.I. et al.* Geological Map of Southeastern Fennoscandia Scale 1:750,000: New Approaches to Compilation // Proceedings of Karelian Research Centre RAS. Precambrian Geology Series. 2017. No.2. Pp. 3–41. DOI: 10.17076/geo444
10. Kostomuksha Ore District (Geology, Deep Structure and Minerageny). Gorkovets V.Ya., Sharov N.V. (eds.). Petrozavodsk: KarRC RAS. 2015. 322 p.
11. *Slabunov A.I., Kervinen A.V., Nesterova N.S.* Zircon from banded iron formation as a sensitive indicator of its polychronous background: a case study on the Kostomuksha greenstone belt, Karelian Craton. Fennoscandian Shield // International Geology Review. 2024. V. 66. No. 6. Pp. 1321–1333. DOI:10.1080/00206814.2023.2248501
12. *Myskova T.A., Milkevich R.I., Lvov P.A. et al.* Neoarchean Volcanics of the Khedozero-Bolshozero Greenstone Structure in Central Karelia: Composition, Age and Tectonic Setting // Stratigraphy and Geological Correlation. 2020. V. 28. No. 2. Pp. 3–32. DOI: 10.31857/S0869592X20020040
13. *Slabunov A.I., Nesterova N.S., Egorov A.V. et al.* Geochemistry, Zircon Geochronology and Age of the Archean Iron Formation of the Kostomuksha Greenstone Belt, Karelian Craton, Fennoscandian Shield // Geochemistry International. 2021. V. 66. No. 4. Pp. 291–307. DOI: 10.31857/S0016752521040063
14. *Milkevich R.I., Myskova T.A.* Late Archean Metaterrigenous Rocks of Western Karelia (Lithology, Geochemistry, Source Areas) // Lithology and Mineral Resources. 1998. No. 2. Pp. 177–194.
15. *Slabunov A.I., Nesterova N.S., Maksimov O.A.* .Geochemistry and Formation Conditions of Mesoarchean Banded Iron Formation (BIF-1) of the Kostomuksha Greenstone Belt, Karelian Craton // Geochemistry International. 2024. V. 69. No. 3. Pp. 28–50. DOI: 10.1134/S0016702924030054

16. *Kozhevnikov V.N.* Archean Greenstone Belts of the Karelian Craton as Accretionary Orogens. Petrozavodsk. 2000. 223 p.

17. *Mudruk S.V., Nesterova N.S., Maksimov O.A.* Structural Analysis of Archean Conglomerates of the Kostomuksha Greenstone Belt (Fennoscandian Shield): First Results // Proceedings of the Fersman Scientific Session of the GI KSC RAS. 2024. 21. Pp. 181–189. DOI: 10.31241/FNS.2024.21.022

18. *Ludwig K.R.* Isoplot v.4.15: A geochronological Toolkit for Microsoft Excel. Special Publication No.4. Berkeley Geochronology Center. 2008.

19. *Järvinen V., Karampelas N., Rämö O.T* . Secular change of tectonic setting in the Archean Takanen greenstone belt, northeastern Karelia Province, Fennoscandian Shield // Bulletin of the Geological Society of Finland. 2023. V. 95. No.2. Pp. 107–134. https://doi.org/10.17741/bgsf/95.2.002

20. *Lehtonen E., Heilimo E., Halkoaho T., Kapyaho A. Holtta P.* U-Pb geochronology of Archaean volcanic-sedimentary sequences in the Kuhmo greenstone belt, Karelia Province – Multiphase volcanism from Meso- to Neoarchaean and a Neoarchaean depositional basin? // Precambrian Research. 2016. V. 275. Pp. 48–69. DOI:10.1016/j.precamres.2015.12.002